Title

Epoxyeicosatrienoic Acids Prevent Cisplatin-Induced Renal Apoptosis through a p38 Mitogen-Activated Protein Kinase–Regulated Mitochondrial Pathway

Journal

Molecular Pharmacology, 84(6)

ISSN

0026-895X

Authors

Liu, Yingmei
Lu, Xiaodan
Nguyen, Sinh
et al.

Publication Date

2013-12-01

DOI

10.1124/mol.113.088302

Peer reviewed

1521-0111/84/6/925–934$25.00
MOLECULAR PHARMACOLOGY

http://dx.doi.org/10.1124/mol.113.088302
Mol Pharmacol 84:925–934, December 2013

Epoxyeicosatrienoic Acids Prevent Cisplatin-Induced Renal Apoptosis through a p38 Mitogen-Activated Protein Kinase–Regulated Mitochondrial Pathway[S]

Yingmei Liu, Xiaodan Lu, Sinh Nguyen, Jean L. Olson, Heather K. Webb, and Deanna L. Kroetz

Departments of Bioengineering and Therapeutic Sciences (Y.L., X.L., S.N., D.L.K.) and Anatomic Pathology (J.L.O.), University of California San Francisco, San Francisco, California; and Arête Therapeutics, Hayward, California (H.K.W.)

Received July 5, 2013; accepted October 2, 2013

ABSTRACT

Soluble epoxide hydrolase (sEH) catalyzes the conversion of epoxyeicosatrienoic acids into less active eicosanoids, and inhibitors of sEH have anti-inflammatory and antiapoptotic properties. Based on previous observations that sEH inhibition attenuates cisplatin-induced nephrotoxicity by modulating nuclear factor-κB signaling, we hypothesized that this strategy would also attenuate cisplatin-induced renal apoptosis. Inhibition of sEH with AR9273 [1-adamantan-1-yl-3-(1-methylsulfonyl-piperidin-4-yl-urea)] reduced cisplatin-induced apoptosis through mechanisms involving mitochondrial apoptotic pathways and by reducing reactive oxygen species. Renal mitochondrial Bax induction following cisplatin treatment was significantly decreased by treatment of mice with AR9273 and these antiapoptotic effects involved p38 mitogen-activated protein kinase signaling. Similar mechanisms contributed to reduced apoptosis in *Ephx2*$^{-/-}$ mice treated with cisplatin. Moreover, in pig kidney proximal tubule cells, cisplatin-induced mitochondrial trafficking of Bax and cytochrome *c*, caspase-3 activation, and oxidative stress are significantly attenuated in the presence of epoxyeicosatrienoic acids (EETs). Collectively, these in vivo and in vitro studies demonstrate a role for EETs in limiting cisplatin-induced renal apoptosis. Inhibition of sEH represents a novel therapeutic strategy for protection against cisplatin-induced renal damage.

Introduction

Cisplatin is a widely used chemotherapeutic for the treatment of solid tumors. A dose-limiting toxicity associated with cisplatin treatment is acute kidney injury (Pabla and Dong, 2008). Cisplatin treatment can lead to tubular cell injury and death, resulting in the loss of renal function. Extensive studies have shown both inflammatory and apoptotic mechanisms for cisplatin-induced acute kidney injury (Ramesh and Reeves, 2002; Zhang et al., 2007; Pabla and Dong, 2008, 2012; Pabla et al., 2009). Numerous renoprotective strategies have been proposed that target key signaling pathways involved in cisplatin-induced necrosis and apoptosis, including tumor necrosis factor-α (TNF-α), caspases, and mitogen-activated protein kinases (MAPKs) (Pabla and Dong, 2008). A novel renoprotective strategy recently proposed by our laboratory is modulation of cytochrome P450 (P450) renal eicosanoid degradation by soluble epoxide hydrolase (sEH) (Liu et al., 2012).

Epoxyeicosatrienoic acids (EETs) are products of CYP2C- and CYP2J-mediated metabolism of arachidonic acid (Kroetz and Zeldin, 2002; Spector et al., 2004; Wang et al., 2010). EETs are further metabolized by sEH to dihydroxyeicosatrienoic acids (DHETs). The EET eicosanoids are associated with a diverse set of biologic functions, including anti-inflammatory and vasodilatory effects (Yang et al., 2007; Marino, 2009; Wang et al., 2010). Modulation of EET levels by inhibition of sEH has been proposed as a novel therapeutic approach for the treatment of hypertension, renal disease, inflammation, pain, and atherosclerosis (Wang et al., 2010). In a mouse model of cisplatin-induced nephrotoxicity, genetic or pharmacological inhibition of sEH markedly increased plasma epoxylipid levels while attenuating renal damage and inflammation in a nuclear factor (NF)-κB–dependent manner (Liu et al., 2012).

The ability of EETs to block apoptosis in cell culture (Jiang et al., 2005; Yang et al., 2007; Dhanasekaran et al., 2008;

This work was supported by the University of California [Discovery Grant Bio06-1-576]; the National Institutes of Health National Institute of Diabetes and Digestive and Kidney Diseases [Grant R01-DK084147]; and in part by Arête Therapeutics.
dx.doi.org/10.1124/mol.113.088302.
[S] This article has supplemental material available at molpharm.aspetjournals.org.

ABBREVIATIONS: AC-DEVD-CHO, *N*-acetyl-L-α-aspartyl-L-α-glutamyl-*N*-(2-carbonyl-1-formylethyl)-L-valinamide; AR9273, 1-adamantan-1-yl-3-(1-methylsulfonyl-piperidin-4-yl-urea); DAPI, 4′,6-diamidino-2-phenylindole; DCF, 2′,7′-dichlorodihydroxyfluorescein; DCFH-DA, 2′,7′-dichlorodihydrofluorescin diacetate; EET, epoxyeicosatrienoic acid; EpETE, epoxyeicosatetraenoic acid; GAPDH, glyceraldehyde-3-phosphate dehydrogenase; LLC-PK1, pig kidney proximal tubule cells; MAPK, mitogen-activated protein kinase; MS-PPOH, *N*-(methylsulfonyl)-2-(2-propynyloxy)-benzenehexanamide; P450, cytochrome P450; PBS, phosphate-buffered saline; ROS, reactive oxygen species; SB203580, 4-(4′-fluorophenyl)-2-(4′-methylsulfinylphenyl)-5-(4′-pyridyl)-imidazole; sEH, soluble epoxide hydrolase; SOD, superoxide dismutase; TNF-α, tumor necrosis factor-α; TNFR, tumor necrosis factor-α receptor.

Bodiga et al., 2009; Chen et al., 2009, 2011; Ma et al., 2010, 2012; Batchu et al., 2011; Liu et al., 2011; Zhao et al., 2012) suggests that the renoprotective properties of sEH inhibition might also be related to their effects on cisplatin-induced apoptosis. The antiapoptotic effects of EETs have been linked to phosphoinositide 3-kinase/protein kinase B and MAPK signaling pathways (Yang et al., 2007; Dhanasekaran et al., 2008; Chen et al., 2009, 2011; Batchu et al., 2011; Liu et al., 2011; Zhao et al., 2012). TNF-α signaling through both tumor necrosis factor-α receptor (TNFR)1 and TNFR2 (Ramesh and Reeves, 2003; Tsuruya et al., 2003) and the production of reactive oxygen species (ROS) (Yao et al., 2007; El-Beshbishy et al., 2011) are implicated in the apoptotic effects of cisplatin. Cisplatin also induces apoptosis through the intrinsic or mitochondrial pathway, resulting in Bax accumulation in mitochondria, cytochrome *c* release, and caspase activation (Huang et al., 2001; Lee et al., 2001; Park et al., 2002). In our recent study, inhibition of sEH resulted in increases in epoxylipid levels and concomitant decreases in cisplatin-induced apoptosis (Liu et al., 2012). The mechanism for this antiapoptotic effect of sEH inhibition is the focus of this study.

Materials and Methods

Reagents. Cisplatin, DAPI (4′,6-diamidino-2-phenylindole), Mitochondrial Isolation Kit, and Caspase-3 Activity Assay Kit were purchased from Sigma-Aldrich (St. Louis, MO). The sEH chemical inhibitor AR9273 [1-adamantan-1-yl-3-(1-methylsulfonyl-piperidin-4-yl-urea)] was synthesized and kindly provided by Arête Therapeutics (Hayward, CA). MS-PPOH [*N*-(methylsulfonyl)-2-(2-propynyloxy)-benzenehexanamide] was purchased from Cayman Chemical (Ann Arbor, MI). The ApoAlet Caspase Profiling Plate was purchased from Clontech Laboratories, Inc. (Fitchburg, WI) and the Caspase-9 Activity Assay Kit was from Chemicon International, Inc. (Temecula, CA). Primary antibodies against phosphorylated- or total-p38 MAPK, precaspase-9, cleaved caspase-3, and cytochrome *c* were purchased from Cell Signaling Technology (Danvers, MA). Innocyte Flow Cytometric Cytochrome *c* Release Kit and Anti-Bax were products of EMD Millipore (Temecula, CA), and the activated caspase-3 antibody and superoxide dismutase (SOD) Activity Assay kit were from Abcam (Cambridge, MA). OxiSelect Intracellular and In Vitro ROS assay kits were purchased from Cell Biolabs, Inc. (San Diego, CA). GAPDH (glyceraldehyde-3-phosphate dehydrogenase), goat anti-rabbit Alexa Fluor 594 antibody, and goat anti-mouse or goat anti-rabbit Alexa Fluor 488 antibody were from Life Technologies (Grand Island, NY). Infrared IRDye-labeled secondary antibodies for Western blot were from Li-Cor, Inc. (Lincoln, NE). PARIS reagents were purchased from Ambion (Austin, TX). BCA Assay Kit was purchased from Pierce (Rockford, IL).

Animal Experiments. C57BL/6 mice were purchased from Charles River Laboratories (Wilmington, MA). In all studies, 8- to 10-week-old male mice weighing 20–25 g were used. Animal experiments were conducted with adherence to the NIH Guide for the Care and Use of Laboratory Animals and were approved by the Animal Care and Use Committee of the University of California, San Francisco. Cisplatin and AR9273 were freshly prepared in sterile saline or 1% carboxymethylcellulose/0.1% Tween 80, respectively. C57BL/6 mice were given 100 mg/kg AR9273 or vehicle daily by oral gavage starting one day prior to cisplatin treatment and continuing for 5 days. A single dose of 20 mg/kg cisplatin or an identical volume of sterile saline was administered to mice by intraperitoneal injection. Mice were sacrificed 24, 48, or 72 hours postcisplatin treatment (30 minutes following the last dose of AR9273) and the kidneys were flash frozen and stored at −80°C until analyzed.

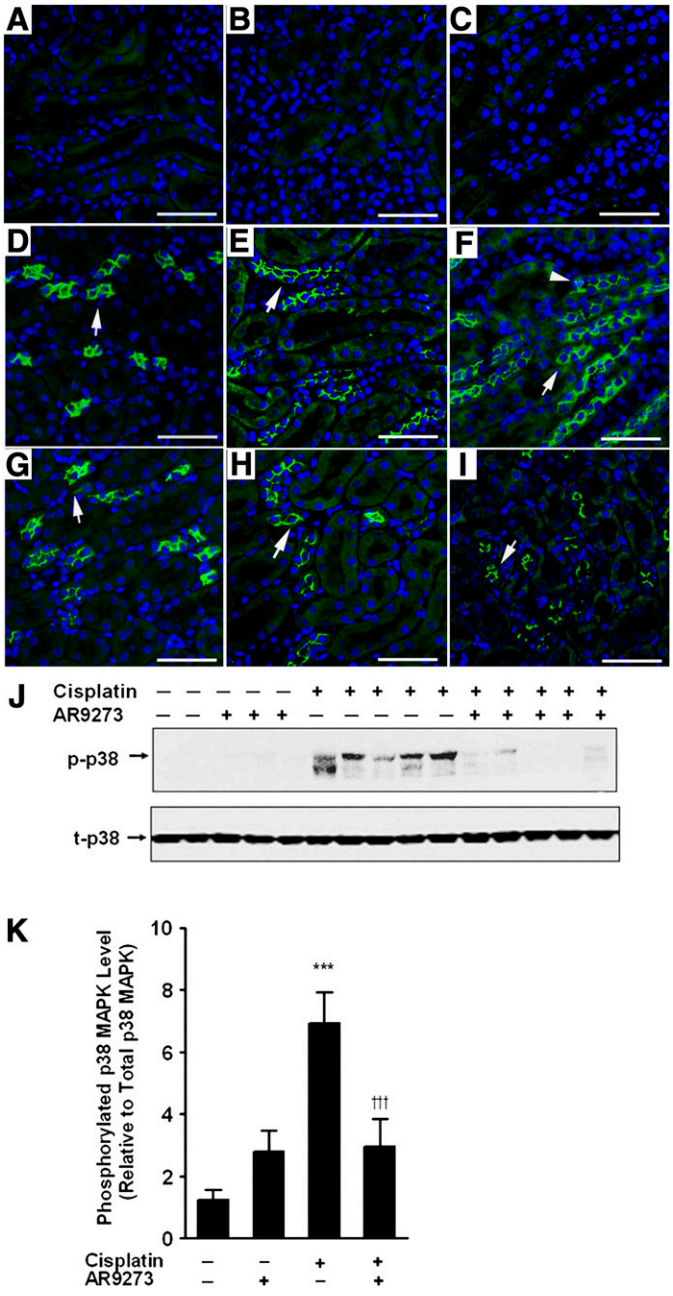

Fig. 1. sEH inhibition attenuates cisplatin-induced p38 MAPK signaling in vivo. Paraffin-embedded kidneys (3 μm) were immunostained with an antibody against phospho-p38 MAPK (bright green) and the nuclei were labeled with DAPI (blue). Cytosolic phosphorylated-p38 MAPK (green) is noted with arrows and nuclear localization of phosphorylated-p38 MAPK (turquoise) is marked with arrowheads. (A and B) Kidneys from saline- and AR9273 (100 mg/kg daily by oral gavage)-treated mice collected at 72 hours and stained with antiphospho-p38 MAPK. (C) Kidney from a cisplatin-treated (single 20 mg/kg dose) mouse collected at 72 hours and stained with rabbit serum. (D–F) Cisplatin-treated mice (G–I) and cisplatin plus AR9273–treated mice at 24 (D and G), 48 (E and H) and 72 hours (F and I), respectively. The bar indicates 50 μm. In J, renal lysates prepared from kidneys harvested 72 hours after cisplatin treatment were subjected to SDS-PAGE followed by immunoblotting for phosphorylated-p38 MAPK (p-p38; upper) or total-p38 MAPK (t-p38; lower). Phosphorylated-p38 MAPK was quantified using laser densitometry and is expressed relative to total-p38 MAPK levels (K). The values shown are the mean ± S.D. for three samples per group and are representative of five independent measurements. Significant differences are indicated: $^{***}P < 0.001$ cisplatin compared with saline control; $^{\dagger\dagger\dagger}P < 0.001$ cisplatin compared with cisplatin plus AR9273.

Immunohistochemistry. Paraffin-embedded kidneys were sectioned at 3 μm. Paraffin was removed with two washes with 100% xylene for 3 minutes, followed by 1:1 xylene/ethanol for 3 minutes, 100% ethanol for 3 minutes, 95% ethanol for 3 minutes, 70% ethanol for 3 minutes, 50% ethanol for 3 minutes and a final wash with tap water. Kidney sections were stained with H&E using standard methods. The renal injury was scored by counting the number of apoptotic tubules in the cortex and outer stripe of the outer medulla in 20 high-power fields at 400× magnification. The analysis was performed by a board-certified pathologist without knowledge of the experimental groups. Immunohistochemistry was performed by incubating kidney sections overnight at 4°C with antibodies against phosphorylated-p38 MAPK or the active form of caspase-3. A species-appropriate serum was used as the staining control on 72-hour cisplatin-treated mice. After three washes with phosphate-buffered saline (PBS), the slides were incubated with a fluorescently conjugated secondary antibody for 1 hour at room temperature or for overnight at 4°C, protected from light. After three washes with PBS, images were captured using a Retiga CCD-cooled camera and associated QCapture Pro software (Qimaging, Surrey, BC, Canada).

Cell Culture and Immunocytochemistry. Pig kidney proximal tubule (LLC-PK1) cells were purchased from American Type Culture Collection (Manassas, VA) and cultured in M199 medium supplemented with 10% fetal bovine serum and 1% penicillin-streptomycin. In brief, LLC-PK1 cells were treated with or without 3 μM EETs in the presence or absence of 10 μM SB203580 [4-(4′-fluorophenyl)-2-(4′-methylsulfinylphenyl)-5-(4′-pyridyl)-imidazole], 500 μM *N*-acetylcysteine, 10 μM AR9273, or 3 μM MS-PPOH for 1 hour prior to 50-μM–cisplatin treatment. After 20 hours of cisplatin treatment, the cells were washed with cold PBS and fixed with 4% paraformaldehyde for 20 minutes at room temperature. Cells were then washed three times with PBS, and incubated with a primary antibody against cytochrome *c*, phosphorylated- or total-p38 MAPK, or the active form of Bax in a way similar to that described above. LLC-PK1 cell fractions for cytochrome *c* immunocytochemistry were specifically isolated and fixed with Innocyte Flow Cytometric Cytochrome *c* Release Kit (EMD Millipore) reagents according to the manufacturer's instructions.

Preparation of Mitochondrial Fractions. Mitochondrial fractions were isolated with a mitochondrial isolation kit (Sigma-Aldrich). In brief, at the conclusion of each treatment, kidneys or cells were washed with cold PBS and centrifuged at 600*g* for 5 minutes. Tissue or cell pellets were incubated with Extraction Buffer A for 10 minutes on ice, homogenized for 10–30 strokes and centrifuged at 600*g* for 10 minutes. Supernatants were removed and centrifuged at 11,000*g* for 10 minutes. The mitochondrial fractions were resuspended as suggested by the manufacturer. All centrifugations were carried out at 4°C.

Western Blot. Kidney tissues were lysed with Ambion PARIS reagents. Protein concentrations were quantified using a BCA assay (Pierce). Protein aliquots from each sample were separated by SDS-PAGE and transferred to a nitrocellulose membrane. The membranes were blocked with PBS-0.1% Tween 20 buffer containing 5% nonfat dried milk for 1 hour at room temperature and then probed overnight at 4°C with a primary antibody against phosphorylated- or total-p38 MAPK, GAPDH, precaspase-9, cleaved caspase-3, or Bax-NT. Membranes were rinsed three times with PBS–0.1% Tween 20, followed by incubation with a secondary antibody for 1 hour at room temperature or for overnight at 4°C. Proteins were detected and expression levels were analyzed with Li-Cor Odyssey Software.

Caspase-2, -3, -8, and -9 Activity Enzyme Immunoassay. Lysates from renal tissue and LLC-PK1 cells were used to detect caspase-3, (Sigma-Aldrich), caspase-9 (Chemicon), and caspases-8 and -2 (Clontech) activities. The assays were performed exactly as described by the manufacturers.

Superoxide Dismutase Activity Assay. Briefly, renal or cell lysates were homogenized in ice-cold 0.1 M Tris-HCl containing 0.5% Triton X-100, 5 mM β-mercaptoethanol, and 0.1 mg/ml phenylmethanesulfonyl fluoride and centrifuged at 14000*g* for 5 minutes at 4°C to remove cell debris. The assay was performed exactly as described by the manufacturer (Abcam, Cambridge, MA). After incubation at 37°C for 20 minutes absorbance was measured at 450 nm using a microplate reader.

Reactive Oxygen Species Quantification. Reactive oxygen species were measured using a fluorescence-based assay according to the manufacturer's protocol. The cell-permeable fluorogenic probe DCFH-DA (2′,7′-dichlorodihydrofluorescin diacetate) diffuses into cells and is deacetylated by cellular esterases to the nonfluorescent 2′,7′-dichlorodihydrofluorescin, which is rapidly oxidized to highly fluorescent DCF (2′,7′-dichlorodihydroxyfluorescein) by ROS. In the LLC-PK1

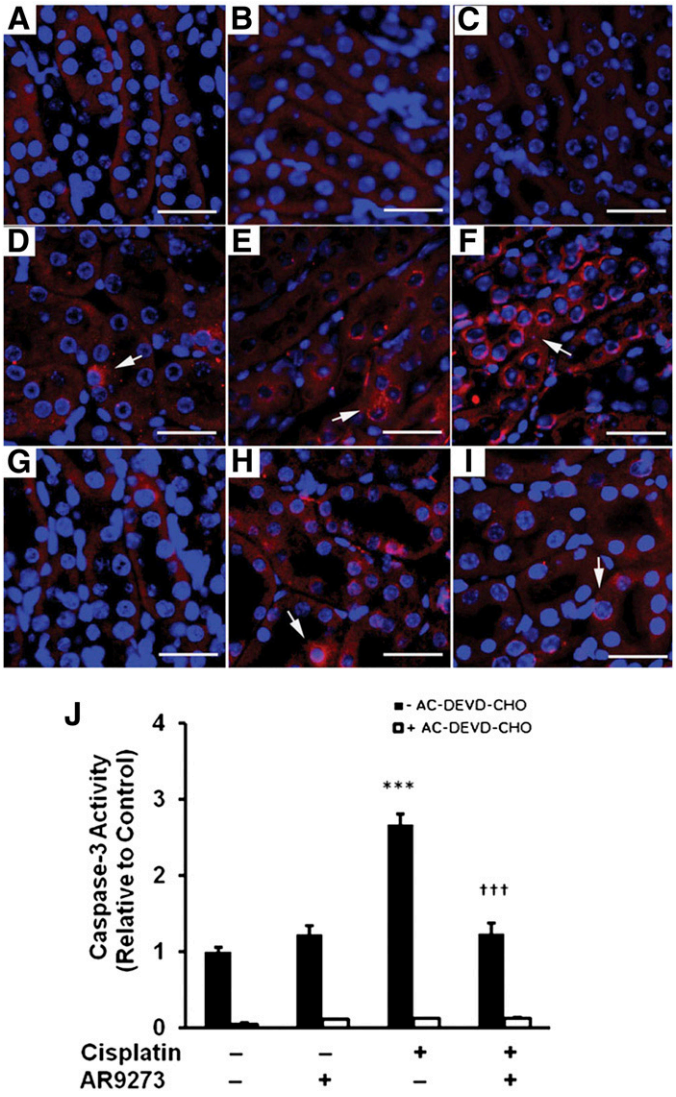

Fig. 2. sEH inhibition attenuates cisplatin-induced activation of caspase-3 in vivo. Paraffin-embedded kidneys (3 μm) were immunostained for an activated form of caspase-3 (bright red) and DAPI (blue). The arrows indicate cleaved caspase-3 and the bar denotes 50 μm. Activated caspase-3 is absent in kidneys collected at 72 hours from saline (A) and AR9273 (B) treated mice; C is kidney from mice treated for 72 hours with cisplatin stained with rabbit serum. (D–F) Representative kidney sections from cisplatin treated mice while G–I are representative kidney sections from cisplatin plus AR9273–treated mice at 24 (D and G), 48 (E and H), and 72 hours (F and I), respectively. Caspase-3 activity was measured in renal lysates in the absence and presence of a caspase-3 inhibitor (AC-DEVD-CHO) using an enzyme immunoassay. Values shown in J are the mean ± S.D. from three samples. Significant differences are indicated: $^{***}P < 0.001$ cisplatin compared with saline control; $^{\dagger\dagger\dagger}P < 0.001$ cisplatin compared with cisplatin plus AR9273.

studies, cell culture plates were precoated with a 1× DCFH-DA/media solution for 30–60 minutes, washed three times with Dulbecco's PBS and used as described above. ROS levels were determined using DCF standards supplied by the manufacturer (Cell Biolab, San Diego, CA).

Terminal Deoxynucleotidyl Transferase–Mediated Digoxigenin-Deoxyuridine Nick-End Labeling Assay. A terminal deoxynucleotidyl transferase–mediated digoxigenin-deoxyuridine nick-end labeling assay was performed with an in situ cell-death detection kit, TMR Red (Roche Diagnostics, Mannheim, Germany). Cells were seeded in 8-well chambers and were treated with cisplatin (50 μM) in the presence or absence of the P450 inhibitor MS-PPOH (3 μM) or purified 11,12-EET (3 μM) for 20 hours. Cells were then washed with cold PBS and stained following the manufacturer's directions. DAPI staining was used for identifying nuclei. Apoptotic cells were counted in five random fields at 200× magnification in triplicate samples.

Statistics. Values are expressed as mean ± S.D. as indicated in the figure legends. Differences between treatments were analyzed by analysis of variance followed by Bonferroni post-hoc multiple comparison testing using GraphPad Prism 5. A $P < 0.05$ was considered significant. All experiments were repeated two or three times and representative results are shown.

Results

sEH Inhibition Attenuates Cisplatin-Induced Apoptotic Signaling through p38 MAPK Activation In Vivo. We have previously reported that pharmacological or genetic inhibition of sEH attenuates cisplatin-induced apoptosis in the kidney (Liu et al., 2012), although the mechanism for this antiapoptotic effect was not determined. Here, we investigated the effect of pharmacological inhibition of sEH on p38 MAPK signaling. Cisplatin treatment caused tubular damage and apoptosis in the cortex and outer stripe of the medulla that was significantly attenuated by treatment with the sEH inhibitor AR9273 (Supplemental Fig. 1). Apoptotic tubules were visible by 48 hours after cisplatin treatment and increased further by 72 hours (Supplemental Fig. 1, A–I). Quantification of EETs and epoxyocatadecenoic acids and their corresponding diols in plasma confirmed the inhibition of sEH in vivo by AR9273 treatment (Supplemental Fig. 2). Saline- or AR9273-treated mice had no detectable phosphorylated-p38 MAPK in the kidney (Fig. 1, A and B). In contrast, cisplatin treatment was associated with induction of p38 MAPK phosphorylation within 24 hours of administration and phosphorylation of p38 MAPK increased dramatically over the 72-hour period following cisplatin treatment (Fig. 1, D–F). Inhibition of sEH with AR9273 significantly attenuated p38 MAPK phosphorylation induced by cisplatin (Fig. 1, G–I). Western blots of renal tissue collected 72 hours after cisplatin treatment confirmed the attenuation of cisplatin-induced p38 MAPK phosphorylation by AR9273 treatment (Fig. 1, J and K). Similar results were observed in mice with a genetic deletion of *Ephx2*. Cisplatin significantly induced the phosphorylation of p38 MAPK in $Ephx2^{+/+}$ mice (Supplemental Fig. 3, B, D, F, and G) but not in $Ephx2^{-/-}$ mice (Supplemental Fig. 3, A, C, F, and G).

sEH Inhibition Prevents Cisplatin-Induced Activation of Caspase-3 In Vivo. In apoptotic cells, caspase-3 has been detected in the cytosol (Samali et al., 1999). In the kidneys of cisplatin-treated mice, activated caspase-3 is detected in the cytosol within 24 hours of treatment and increases dramatically over the 72-hour period following cisplatin treatment (Fig. 2, A–F). Inhibition of sEH with AR9273 results in significant attenuation of the activated caspase-3 levels that is most evident at 72 hours following cisplatin administration (Fig. 2, G–I). Consistent with the immunohistochemistry results, cisplatin treatment resulted in activation of caspase-3 that was attenuated by AR9273 treatment (Fig. 2J). Activation of caspase-3 in renal lysates from cisplatin-treated mice was prevented by the caspase-3 inhibitor AC-DEVD-CHO (*N*-acetyl-L-α-aspartyl-L-α-glutamyl-*N*-(2-carbonyl-1-formylethyl)-L-valinamide).

sEH Inhibition Attenuates the Intrinsic Mitochondrial Apoptotic Pathway In Vivo. Cisplatin-induced apoptosis has been previously associated with both an intrinsic mitochondrial and an extrinsic death–receptor pathway (Pabla and Dong, 2008). Cisplatin treatment of C57BL/6 mice caused a decrease in renal cytosolic Bax levels (Fig. 3A) and a corresponding increase in mitochondrial Bax levels (Fig. 3B). Cytosolic Bax levels decreased about 76% (Fig. 3C) while mitochondrial levels increased almost 4-fold (Fig. 3D). This translocation of Bax from the cytosol into the mitochondrial membrane was attenuated by treatment with the sEH inhibitor AR9273. Consistent with the Bax trafficking data, AR9273 treatment attenuated the activation of caspase-9 and -8 (Fig. 4, A and B); this effect was most evident 72 hours following cisplatin treatment. In contrast, caspase-2 was not activated following cisplatin treatment (Fig. 4C). These data support a major role for EETs in preventing cisplatin-induced intrinsic apoptotic pathway activation in vivo.

sEH Inhibition Does Not Regulate Superoxide Dismutase Activity but Attenuates the Increase in ROS In Vivo. Cisplatin is associated with reduced SOD activity and corresponding increases in reactive oxygen species (Yao et al., 2007). Measurement of SOD activity in renal lysates from cisplatin-treated mice showed a significant decrease in activity 48 and 72 hours following treatment and this activity was not restored in the cisplatin-treated mice by chemical inhibition of sEH (Fig. 5A). Consistent with the reduction in SOD activity, cisplatin treatment resulted in a significant

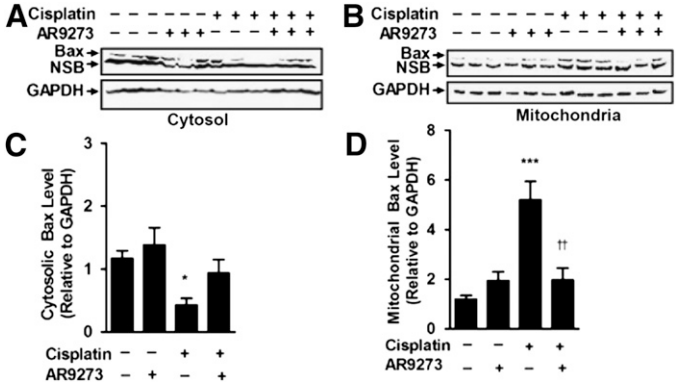

Fig. 3. sEH inhibition attenuates cisplatin-induced Bax translocation into the mitochondria in vivo. Cytosolic (A) and mitochondrial (B) fractions from kidneys harvested 72 hours following cisplatin treatment were subjected to SDS-PAGE and immunoblotting with antibodies against activated Bax (upper) and GAPDH (lower). Bax expression (C and D) was quantified using laser densitometry and expressed relative to GAPDH. Values shown are the mean ± S.D. from three samples. Significant differences are indicated: $^{*}P < 0.01$; $^{***}P < 0.001$, cisplatin compared with saline control; $^{\dagger\dagger}P < 0.01$ cisplatin compared with cisplatin plus AR9273. NSB, nonspecific binding.

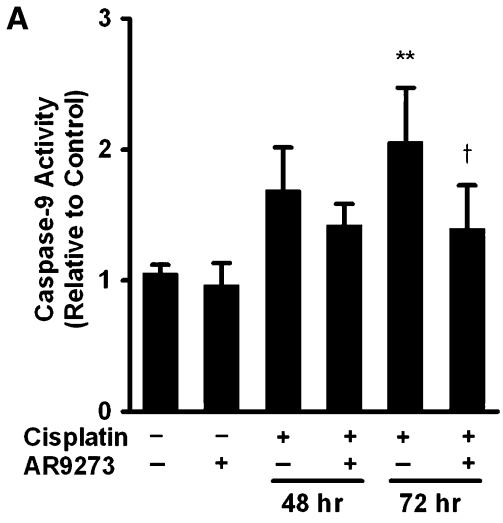

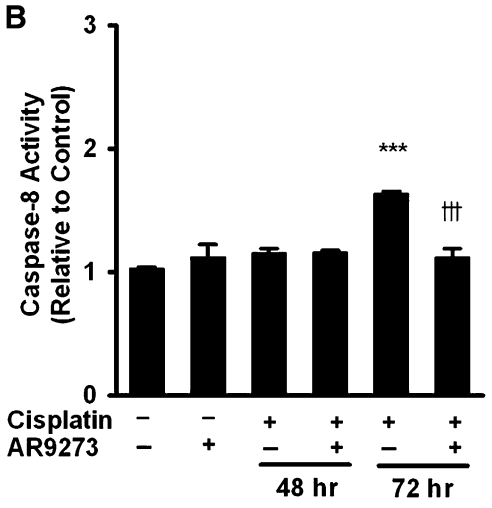

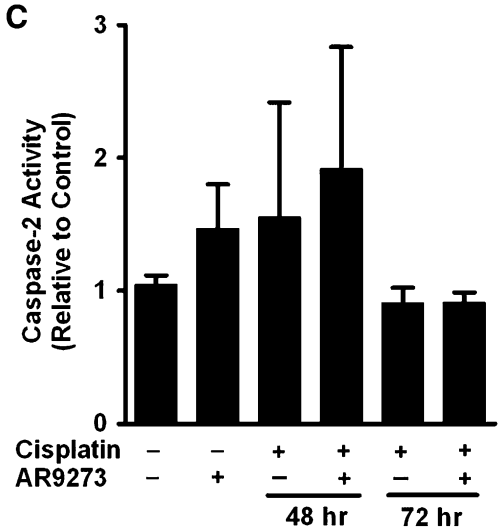

Fig. 4. sEH inhibition attenuates cisplatin-induced caspase activation in vivo. Caspase-9 (A), -8 (B), and -2 (C) activities were measured in renal lysates using enzyme immunoassays. Values shown are the mean ± S.D. from three samples. Significant differences are indicated: $^{**}P < 0.01$; $^{***}P < 0.001$, cisplatin compared with saline control; $^{\dagger}P < 0.05$; $^{\dagger\dagger\dagger}P < 0.001$, cisplatin compared with cisplatin plus AR9273.

increase in renal ROS levels that was attenuated by AR9273 treatment (Fig. 5B). Similar results were found in *Ephx2*$^{-/-}$ mice. The decrease in SOD activity induced by cisplatin treatment was less in *Ephx2*$^{-/-}$ mice compared with the *Ephx2*$^{+/+}$ mice (Supplemental Fig. 4A). Attenuation of the cisplatin-induced increase in ROS levels in *Ephx2*$^{-/-}$ mice compared with *Ephx2*$^{+/+}$ mice was consistent with the effect of sEH inhibitor treatment (Supplemental Fig. 4B).

EETs Protect LLC-PK1 Cells from Cisplatin-Induced Apoptosis. LLC-PK1 cells were used to further explore the renoprotective properties of EETs. A range of EET concentrations was evaluated and 3 μM was chosen for further study since it gave a maximal effect. Cytochrome *c* release from mitochondria is recognized as an early marker of apoptosis. Compared with LLC-PK1 cells treated with vehicle or 11,12-EET (Fig. 6, A and B), cisplatin treatment causes

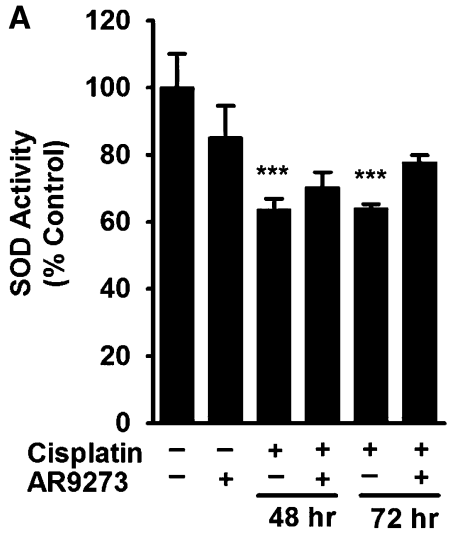

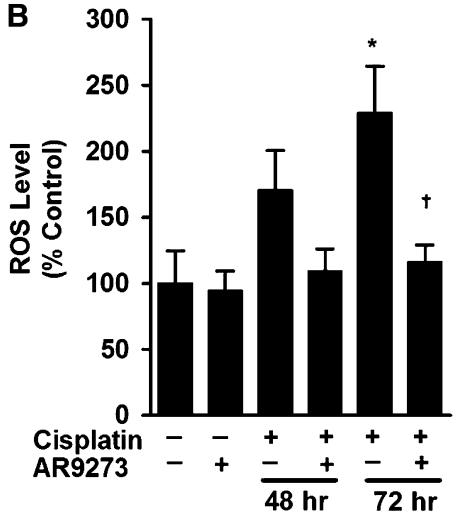

Fig. 5. sEH inhibition does not prevent cisplatin-induced decreases in renal SOD activity but attenuates increases in ROS in vivo. Renal lysates harvested at 48 or 72 hours following cisplatin treatment were analyzed for SOD activity (A) and ROS levels (B). Controls were renal lysates collected at 72 hours from saline- or AR9273-treated mice. Values shown are the mean ± S.D. from three to five samples for each treatment group. Significant differences are indicated: $^{*}P < 0.05$; $^{***}P < 0.001$, cisplatin compared with saline control; $^{\dagger}P < 0.05$, cisplatin compared with cisplatin plus AR9273.

release of cytochrome *c* from the mitochondria (Fig. 6C) and this is prevented by treatment with 11,12-EET (Fig. 6D). Similarly, cisplatin-induced activation of caspase-3 in LLC-PK1 cells is attenuated by 11,12-EET treatment (Fig. 6, E–G). Consistent with an increased caspase-3 activity, there was a trend for a decreased level of precaspase-9 following treatment of LLC-PK1 cells with cisplatin and partial attenuation by 11,12-EET treatment. (Fig. 6, F and H).

The in vivo studies suggest that p38 MAPK signaling is involved in the antiapoptotic effects of sEH inhibition. Treatment of LLC-PK1 cells with cisplatin is associated with phosphorylation of p38 MAPK, and translocation of Bax into the mitochondrial membrane (Fig. 7, A and B). The addition of 11,12- and 14,15-EETs (Fig. 7, E and G), but not 8,9-EET (Fig. 7C), attenuates cisplatin-induced p38 MAPK phosphorylation and Bax translocation. Addition of the p38 MAPK inhibitor SB203580 to EETs resulted in almost complete protection from cisplatin-induced p38 MAPK phosphorylation and Bax translocation (Fig. 7, D, F, and H). Similar results were found if p38 MAPK phosphorylation and Bax were detected by Western blotting (Supplemental Figs. 5 and 6) and the magnitude of the EET effect was similar to that of a potent p38 MAPK inhibitor (Fig. 7, I–K; Supplemental Figs. 5 and 6). Inhibition of endogenous epoxylipids with AR9273 had a similar effect on p38 MAPK phosphorylation and Bax translocation as EET treatment (Supplemental Figs. 5 and 6).

Studies were also carried out using an inhibitor of P450 epoxygenases (MS-PPOH) to lower endogenous EET levels. MS-PPOH itself had no apoptotic effects (Fig. 8, B and H) but showed a trend toward increasing cisplatin-induced apoptosis (Fig. 8, D, E, and H). The ability of P450 epoxygenase inhibition to enhance apoptosis can be suppressed by supplementation with exogenous EETs (Fig. 8, F, G, and H).

Treatment of LLC-PK1 cells with regioisomeric EETs reversed the modest cisplatin-induced decrease in SOD activity (Fig. 9A) and attenuated the increase in cisplatin-induced ROS levels (Fig. 9B). The effect of EETs was similar to treatment with the sEH inhibitor AR9273 or with the ROS scavenger *N*-acetylcysteine (Fig. 9, A and B).

Discussion

Apoptosis or programmed cell death plays an important role in regulating mammalian physiology (Reed, 2002; Hanigan and Devarajan, 2003; Reed et al., 2003). In animal models of cisplatin-induced acute kidney injury, apoptosis is a prominent feature (Ramesh and Reeves, 2002; Zhang et al., 2007; Pabla and Dong, 2008, 2012; Pabla et al., 2009). Treatment with p38 MAPK inhibitors prior to cisplatin significantly decreases apoptosis in vivo and in vitro (Ramesh and Reeves, 2002, 2003, 2005), indicating that p38 MAPK signaling is involved in cisplatin-induced renal injury (Ramesh and Reeves, 2005). Overexpression of P450s significantly protects

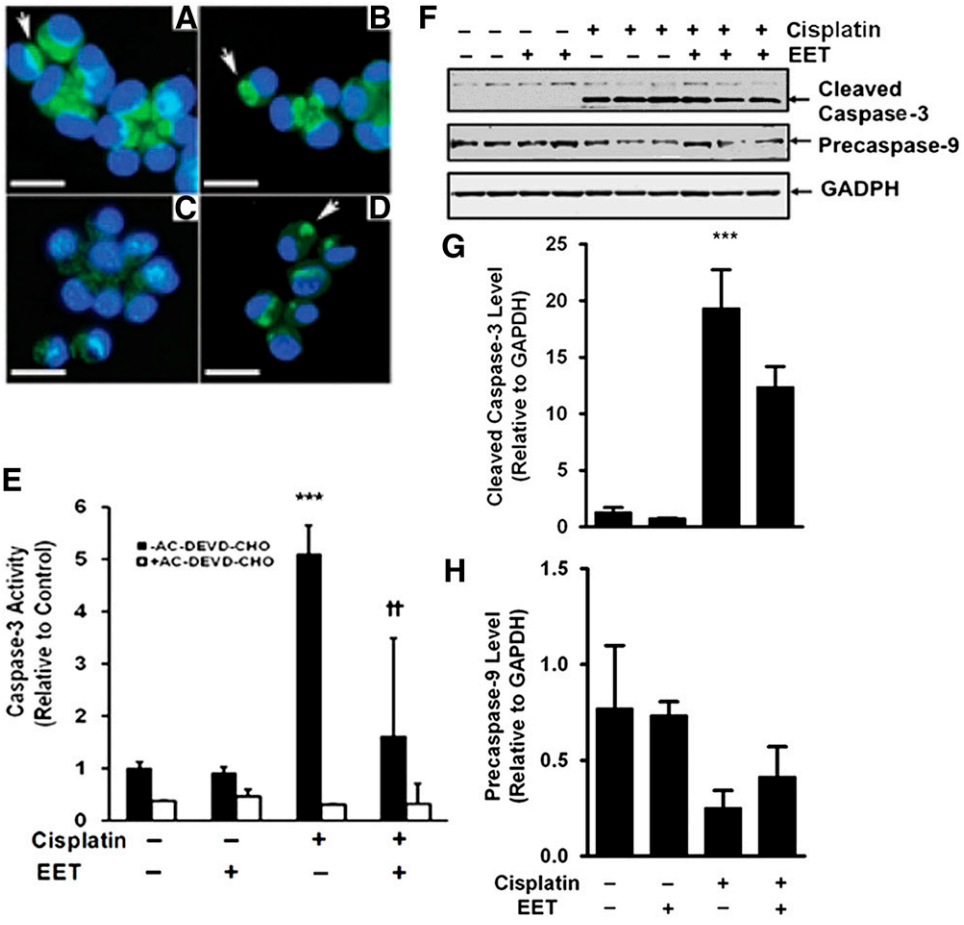

Fig. 6. EETs protect LLC-PK1 cells from cisplatin-induced cytochrome *c* release and caspase-3 activation. LLC-PK1 cells were treated with cisplatin in the absence or presence of 11,12-EET (3 μM). Localization of cytochrome *c* (bright green) was detected by immunocytochemistry (A–D). DAPI staining is blue. Representative images are shown for cells treated with vehicle (A), 11,12-EET (B), cisplatin (C), or cisplatin plus 11,12-EET (D). Mitochondrial cytochrome *c* is labeled with arrows. The bar indicates 10 μm. Caspase-3 activity was measured in cell lysates in the absence and presence of the caspase-3 inhibitor AC-DEVD-CHO with an enzyme immunoassay (E). These results are representative of three independent experiments. Values shown are the mean ± S.D. from three samples. There was no effect of ethanol on caspase activity in the absence or presence of cisplatin (data not shown). Significant differences are indicated: $^{***}P < 0.001$, cisplatin compared with control; $^{\dagger\dagger}P < 0.01$, cisplatin compared with cisplatin plus 11,12-EET. Caspase expression (F) was detected by SDS-PAGE followed by immunoblotting against cleaved caspase-3 (top), precaspase-9 (middle), or GAPDH (bottom). The expression of cleaved caspase-3 (G) and precaspase-9 (H) was quantified by laser densitometry and expressed relative to GAPDH levels. Values shown are the mean ± S.D. from three samples. Significant differences are indicated: $^{***}P < 0.001$ cisplatin compared with vehicle control.

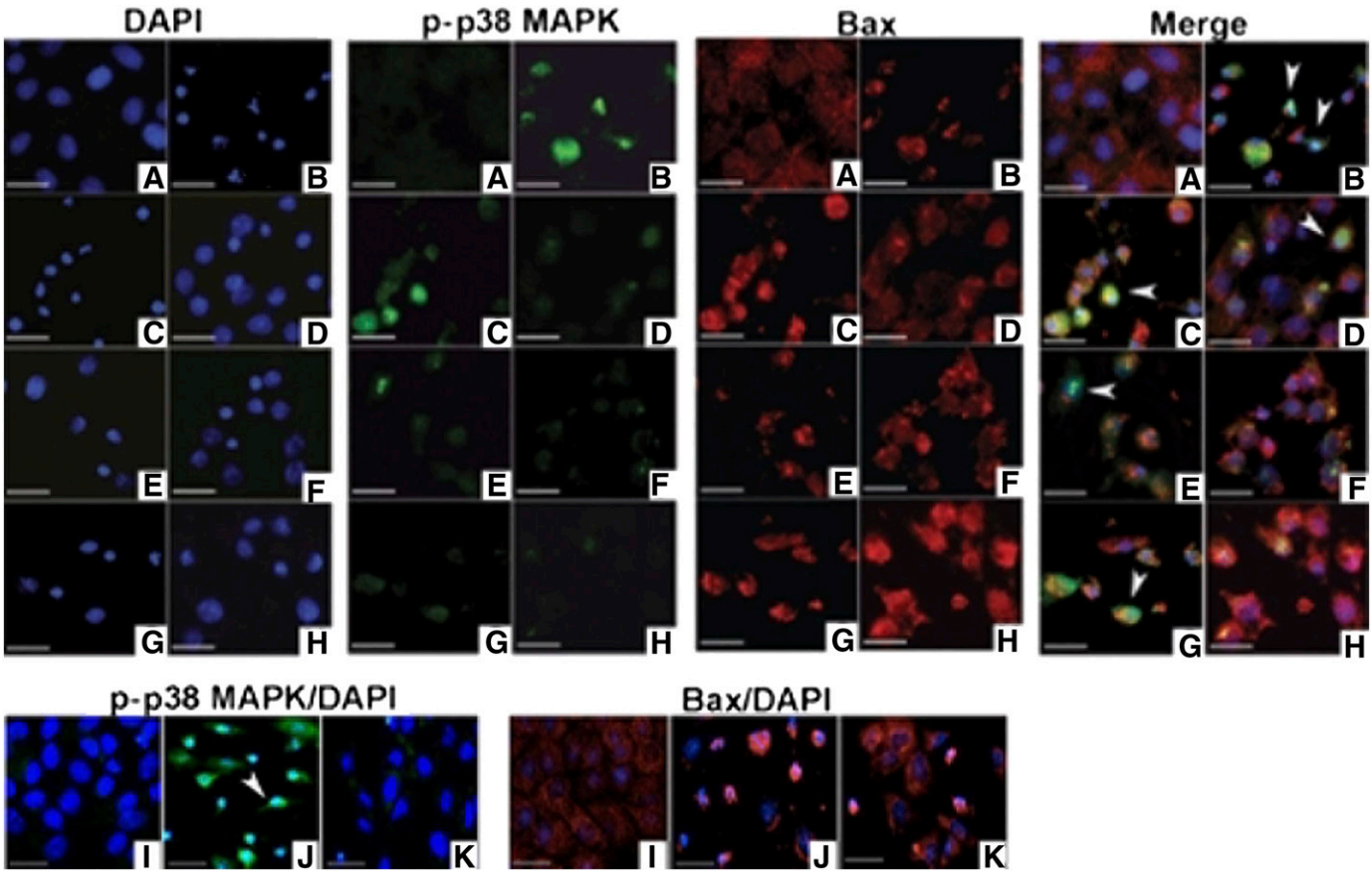

Fig. 7. EETs protect LLC-PK1 cells from cisplatin-induced p38 MAPK activation and Bax mitochondrial trafficking. LLC-PK1 cells were treated with cisplatin in the absence and presence of regioisomeric EETs (3 μM) or the p38 MAPK inhibitor SB203580 (10 μM). Cells were stained with an antibody against phosphorylated-p38 MAPK (green) or an active form of Bax (red). Nuclei were stained with DAPI (blue). Nuclear phosphorylated-p38 MAPK is marked with an arrowhead (turquoise, merged images). Cell treatments were (A) vehicle control, (B) cisplatin, (C) cisplatin plus 8,9-, (E) 11,12-, or (G) 14,15-EET, (D) cisplatin plus 8,9-EET and SB203580, (F) 11,12-EET and SB203580, or (H) 14,15-EET and SB203580, (I) SB203580, (J) cisplatin, and (K) cisplatin plus SB203580. The bar indicates 10 μm.

endothelial cells from TNF-α–induced apoptosis, in part through inhibition of extracellular signal-related kinase dephosphorylation and activation of phosphoinositide 3-kinase/protein kinase B signaling (Yang et al., 2007). Pretreatment with the eicosanoids 17,18-EpETE (17,18-epoxyeicosatetraenoic acid), 14,15-EET and 11,12-EET prevents the phosphorylation of p38 MAPK induced by TNF-α in human bronchi (Morin, 2010) and by As_2O_3 in Tca-8113 cells (Liu et al., 2011). Previous studies have also shown that TNFR1/2–deficient mice are resistant to cisplatin nephrotoxicity and that TNFR2 has a key role in cisplatin-induced apoptosis (Ramesh and Reeves, 2003; Tsuruya et al., 2003). Considering these earlier studies implicating EETs in antiapoptotic effects and our recent finding that inhibition of sEH attenuates cisplatin-induced TNF-α and TNFR1/2 induction (Liu et al., 2012), we hypothesized that increased EET levels resulting from sEH inhibition would protect against cisplatin-induced apoptosis by interfering with p38 MAPK signaling.

Cytosolic p38 MAPK, and to a lesser extent nuclear p38 MAPK, are phosphorylated under apoptotic conditions (Kyriakis and Avruch, 2001; Wood et al., 2009). In the current study, the majority of phosphorylated-p38 MAPK was cytosolic, consistent with previous studies (Raingeaud et al., 1995; Burger et al., 1997; Kyriakis and Avruch, 2001; Wood et al., 2009). Nuclear localization of phosphorylated-p38 MAPK is only found at 72 hours following cisplatin treatment and may indicate more severe apoptosis at this time.

Phosphorylation of p38 MAPK has been coupled to activated caspase-3 (Segreto et al., 2011). Caspases are synthesized as inactive proenzymes and activated by cleavage at specific Asp residues. Caspase-3, -8, and -9 have been detected in the cytosol of apoptotic cells (Zhivotovsky et al., 1999). Our results suggest that sEH inhibition attenuates cisplatin-induced apoptosis largely by modulating caspase-3 activity, although caspase-8 and -9 activities are also affected. The involvement of caspase-3 is consistent with previous reports of cisplatin-induced apoptosis (Zhan et al., 1999; Kaushal et al., 2001) and EET analogs have recently been shown to attenuate cisplatin-induced caspase-3 activity in Wistar-Kyoto rats (Khan et al., 2013). The current studies do not rule out a role for sEH inhibition in modulating caspase-independent events mediating cisplatin-induced renal apoptosis (Cummings and Schnellmann, 2002). sEH inhibition had no effect on cisplatin-induced caspase-2 or -12 activity (data not shown), suggesting that sEH inhibition has minimal effect on endoplasmic reticulum stress-signaling pathways that have been previously associated with cisplatin nephrotoxicity (Pabla and Dong, 2008). In contrast, recent studies in Wistar-Kyoto rats showed a reduction in caspase-12 and other markers of endoplasmic reticulum stress when rats were pretreated with

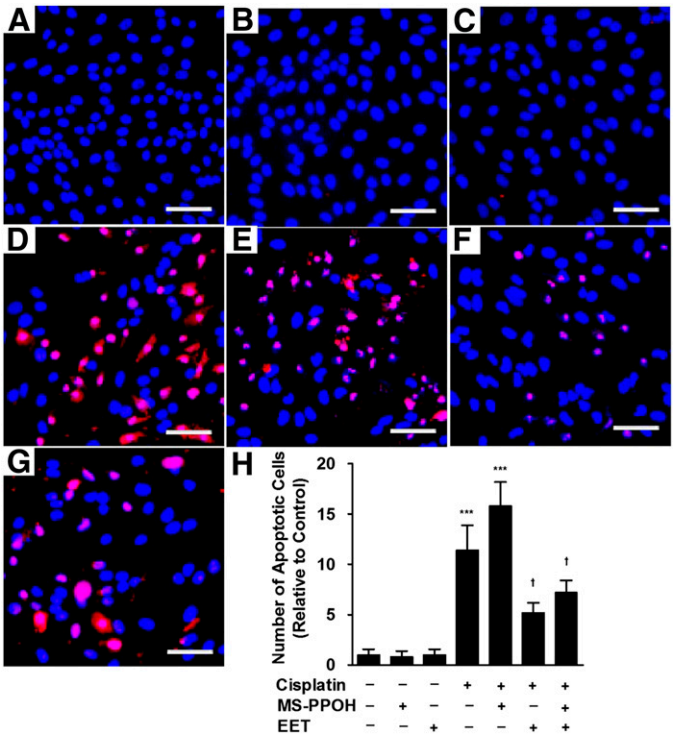

Fig. 8. Inhibition of P450 epoxygenase activity enhances cisplatin-induced apoptosis in LLC-PK1 cells. LLC-PK1 cells were treated with cisplatin in the absence or presence of the P450 epoxygenase inhibitor MS-PPOH (3 μM) or EETs (3 μM). Apoptotic cells were detected by a terminal deoxynucleotidyl transferase–mediated digoxigenin-deoxyuridine nick-end labeling assay and are stained red. Nuclei are indicated by DAPI staining (blue). The bar indicates 25 μm. Representative images are shown for cells treated with (A) vehicle, (B) MS-PPOH, (C) EETs, (D) cisplatin, (E) cisplatin plus MS-PPOH, (F) cisplatin plus EETs, and (G) cisplatin plus MS-PPOH and EETs. The number of apoptotic cells was counted in five random fields at 200× magnification and the values shown are the mean ± S.D. from three samples (H). Significant differences are indicated: ***$P < 0.001$ compared with control; $^{\dagger}P < 0.05$, sample compared with cisplatin alone.

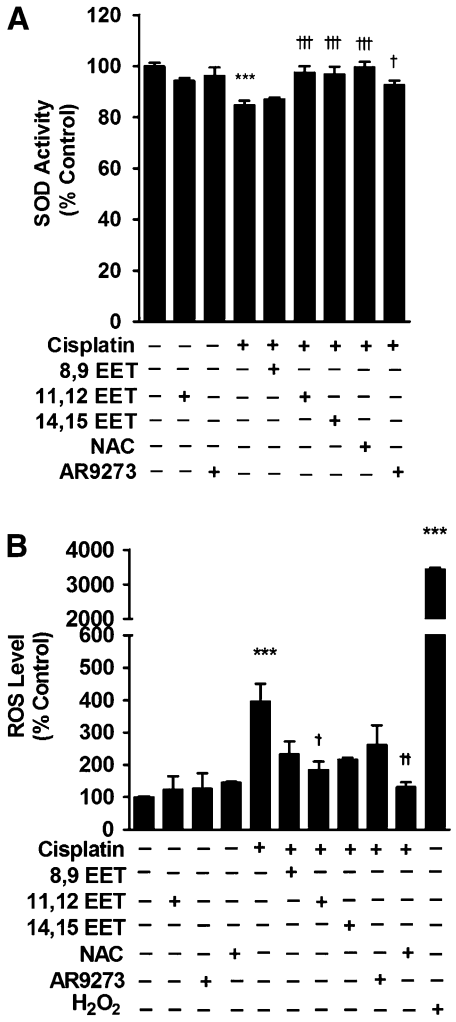

Fig. 9. Treatment of LLC-PK1 cells with EETs or an sEH inhibitor attenuates the effect of cisplatin on SOD activity and levels of ROS. LLC-PK1 cells were treated with cisplatin (50 μM) in the absence or presence of regioisomeric EETs (3 μM), the ROS scavenger *N*-acetylcysteine (NAC; 500 μM) or the sEH inhibitor AR9273 (10 μM). Hydrogen peroxide (H_2O_2; 10 μM), a ROS inducer, was added to cells as a positive control. SOD activity (A) and ROS levels (B) were measured and values shown are the mean ± S.D. from three to five independent samples from each treatment. Significant differences are indicated: ***$P < 0.001$, cisplatin or H_2O_2 compared with control; $^{\dagger}P < 0.05$; $^{\dagger\dagger}P < 0.01$; $^{\dagger\dagger\dagger}P < 0.001$, cisplatin compared with cisplatin plus EETs, AR9273, or NAC alone or in combination.

EET analogs (Khan et al., 2013). Species differences or treatment strategy might account for these differences in EET effects on the endoplasmic reticulum stress pathway.

Both an intrinsic mitochondrial and an extrinsic death–receptor pathway have been associated with cisplatin-induced renal apoptosis and acute kidney injury (Gordon and Gattone, 1986; Pabla and Dong, 2008). The proapoptotic protein Bax is found in the cytosol of healthy cells and moves to the mitochondria upon initiation of apoptosis (Hsu et al., 1997; Wolter et al., 1997). $Bax^{-/-}$ mice were resistant to cisplatin-induced apoptosis (Wei et al., 2007), suggesting that this is a key event in cisplatin nephrotoxicity. In the current in vivo study, treatment with AR9273 significantly attenuated the movement of Bax into the mitochondrial membrane following cisplatin treatment, suggesting that elevated renal EET levels can interfere with Bax trafficking in response to apoptotic signals. Cisplatin has been previously found to induce apoptosis in LLC-PK1 cells (Park et al., 2002; Seth et al., 2005) and these cells were used to confirm a direct effect of EETs on Bax trafficking and p38 MAPK signaling. It has been shown that death signals induce cytochrome *c* release from the mitochondria upstream of caspase-3 (Liu et al., 1996) and caspase-9 (Li et al., 1997) activation. Cisplatin has also been shown to downregulate Bcl2 and induce Bax mRNA in gastric adenocarcinoma cells (Korbakis and Scorilas, 2012). Consistent with the current findings, EET analogs increase the ratio of antiapoptotic to proapoptotic signals in cisplatin-treated rats (Khan et al., 2013). Among the EET regioisomers, 11,12- and 14,15-EET, but not 8,9- EET, have antiapoptotic properties in cisplatin-treated LLC-PK1 cells, an effect that was similar to inhibition of p38 MAPK. Together, these results suggest that EETs attenuate cisplatin-induced renal apoptosis at least in part by inhibiting p38 MAPK phosphorylation upstream of the intrinsic mitochondrial apoptosis pathway.

Cisplatin treatment is associated with a decrease in cellular SOD activity and corresponding increases in levels of reactive oxygen species (Yao et al., 2007; El-Beshbishy et al., 2011). In cells, EETs can upregulate SOD and reduce apoptosis and

cellular toxicity associated with arsenic trioxide treatment (Liu et al., 2011). In the current study, SOD activity did decrease in cisplatin-treated kidneys but sEH inhibition or genetic deletion of *Ephx2* had only a modest effect on this activity. However, direct measurement of reactive oxygen species during sEH inhibition or in *Ephx2*$^{-/-}$ mice is consistent with a role for EETs and possibly other epoxylipids in controlling cisplatin-induced oxidative stress, resulting in reduced apoptosis. Additional properties of EETs beyond the minimal effects on SOD activity likely contribute to the robust change in levels of reactive oxygen species. These findings are consistent with the ability of EET analogs to attenuate signals of oxidative stress in cisplatin-treated rats (Khan et al., 2013).

The current study demonstrates a role for EETs in protection against cisplatin-induced apoptosis through at least two distinct mechanisms. First, sEH inhibition or genetic disruption of *Ephx2* interferes with p38 MAPK signaling upstream of the intrinsic mitochondrial apoptotic pathway. In addition, oxidative stress is reduced by pharmacologic or genetic alteration of sEH activity. Whether EETs also modulate extrinsic signaling pathways implicated in cisplatin-induced renal apoptosis (Pabla and Dong, 2008) will require further study. It is of interest to determine whether sEH inhibition can effectively protect against renal apoptosis induced by other mechanisms, including physical obstruction and ischemia-reperfusion. Inhibition of sEH activity may provide a novel therapeutic strategy for the prevention and treatment of acute kidney injury.

Authorship Contributions

Participated in research design: Liu, Webb, Kroetz.

Conducted experiments: Liu, Lu, Nyugen.

Performed data analysis: Liu, Olson, Kroetz.

Wrote or contributed to the writing of the manuscript: Liu, Olson, Webb, Kroetz.

References

Batchu SN, Lee SB, Qadhi RS, Chaudhary KR, El-Sikhry H, Kodela R, Falck JR, and Seubert JM (2011) Cardioprotective effect of a dual acting epoxyeicosatrienoic acid analogue towards ischaemia reperfusion injury. *Br J Pharmacol* **162**:897–907.

Bodiga S, Zhang R, Jacobs DE, Larsen BT, Tampo A, Manthati VL, Kwok WM, Zeldin DC, Falck JR, and Gutterman DD et al. (2009) Protective actions of epoxyeicosatrienoic acid: dual targeting of cardiovascular PI3K and KATP channels. *J Mol Cell Cardiol* **46**:978–988.

Burger H, Nooter K, Boersma AW, Kortland CJ, and Stoter G (1997) Lack of correlation between cisplatin-induced apoptosis, p53 status and expression of Bcl-2 family proteins in testicular germ cell tumour cell lines. *Int J Cancer* **73**:592–599.

Chen C, Li G, Liao W, Wu J, Liu L, Ma D, Zhou J, Elbekai RH, Edin ML, and Zeldin DC et al. (2009) Selective inhibitors of CYP2J2 related to terfenadine exhibit strong activity against human cancers in vitro and in vivo. *J Pharmacol Exp Ther* **329**:908–918.

Chen C, Wei X, Rao X, Wu J, Yang S, Chen F, Ma D, Zhou J, Dackor RT, and Zeldin DC et al. (2011) Cytochrome P450 2J2 is highly expressed in hematologic malignant diseases and promotes tumor cell growth. *J Pharmacol Exp Ther* **336**: 344–355.

Cummings BS and Schnellmann RG (2002) Cisplatin-induced renal cell apoptosis: caspase 3-dependent and -independent pathways. *J Pharmacol Exp Ther* **302**:8–17.

Dhanasekaran A, Gruenloh SK, Buonaccorsi JN, Zhang R, Gross GJ, Falck JR, Patel PK, Jacobs ER, and Medhora M (2008) Multiple antiapoptotic targets of the PI3K/Akt survival pathway are activated by epoxyeicosatrienoic acids to protect cardiomyocytes from hypoxia/anoxia. *Am J Physiol Heart Circ Physiol* **294**: H724–H735.

El-Beshbishy HA, Bahashwan SA, Aly HA, and Fakher HA (2011) Abrogation of cisplatin-induced nephrotoxicity in mice by alpha lipoic acid through ameliorating oxidative stress and enhancing gene expression of antioxidant enzymes. *Eur J Pharmacol* **668**:278–284.

Gordon JA and Gattone VH, 2nd (1986) Mitochondrial alterations in cisplatin-induced acute renal failure. *Am J Physiol* **250**:F991–F998.

Hanigan MH and Devarajan P (2003) Cisplatin nephrotoxicity: molecular mechanisms. *Cancer Ther* **1**:47–61.

Hsu YT, Wolter KG, and Youle RJ (1997) Cytosol-to-membrane redistribution of Bax and Bcl-X(L) during apoptosis. *Proc Natl Acad Sci USA* **94**:3668–3672.

Huang Q, Dunn RT, 2nd, Jayadev S, DiSorbo O, Pack FD, Farr SB, Stoll RE, and Blanchard KT (2001) Assessment of cisplatin-induced nephrotoxicity by microarray technology. *Toxicol Sci* **63**:196–207.

Jiang JG, Chen CL, Card JW, Yang S, Chen JX, Fu XN, Ning YG, Xiao X, Zeldin DC, and Wang DW (2005) Cytochrome P450 2J2 promotes the neoplastic phenotype of carcinoma cells and is up-regulated in human tumors. *Cancer Res* **65**:4707–4715.

Khan MA, Liu J, Kumar G, Skapek SX, Falck JR, and Imig JD (2013) Novel orally active epoxyeicosatrienoic acid (EET) analogs attenuate cisplatin nephrotoxicity. *FASEB J* **27**:2946–2956.

Kaushal GP, Kaushal V, Hong X, and Shah SV (2001) Role and regulation of activation of caspases in cisplatin-induced injury to renal tubular epithelial cells. *Kidney Int* **60**:1726–1736.

Korbakis D and Scorilas A (2012) Quantitative expression analysis of the apoptosis-related genes BCL2, BAX and BCL2L12 in gastric adenocarcinoma cells following treatment with the anticancer drugs cisplatin, etoposide and taxol. *Tumour Biol* **33**:865–875.

Kroetz DL and Zeldin DC (2002) Cytochrome P450 pathways of arachidonic acid metabolism. *Curr Opin Lipidol* **13**:273–283.

Kyriakis JM and Avruch J (2001) Mammalian mitogen-activated protein kinase signal transduction pathways activated by stress and inflammation. *Physiol Rev* **81**:807–869.

Lee RH, Song JM, Park MY, Kang SK, Kim YK, and Jung JS (2001) Cisplatin-induced apoptosis by translocation of endogenous Bax in mouse collecting duct cells. *Biochem Pharmacol* **62**:1013–1023.

Li P, Nijhawan D, Budihardjo I, Srinivasula SM, Ahmad M, Alnemri ES, and Wang X (1997) Cytochrome c and dATP-dependent formation of Apaf-1/caspase-9 complex initiates an apoptotic protease cascade. *Cell* **91**:479–489.

Liu L, Chen C, Gong W, Li Y, Edin ML, Zeldin DC, and Wang DW (2011) Epoxyeicosatrienoic acids attenuate reactive oxygen species level, mitochondrial dysfunction, caspase activation, and apoptosis in carcinoma cells treated with arsenic trioxide. *J Pharmacol Exp Ther* **339**:451–463.

Liu X, Kim CN, Yang J, Jemmerson R, and Wang X (1996) Induction of apoptotic program in cell-free extracts: requirement for dATP and cytochrome c. *Cell* **86**: 147–157.

Liu Y, Webb HK, Fukushima H, Micheli J, Markova S, Olson JL, and Kroetz DL (2012) Attenuation of cisplatin-induced renal injury by inhibition of soluble epoxide hydrolase involves nuclear factor κB signaling. *J Pharmacol Exp Ther* **341**: 725–734.

Ma J, Zhang L, Han W, Shen T, Ma C, Liu Y, Nie X, Liu M, Ran Y, and Zhu D (2012) Activation of JNK/c-Jun is required for the proliferation, survival, and angiogenesis induced by EET in pulmonary artery endothelial cells. *J Lipid Res* **53**: 1093–1105.

Ma J, Zhang L, Li S, Liu S, Ma C, Li W, Falck JR, Manthati VL, Reddy DS, and Medhora M et al. (2010) 8,9-Epoxyeicosatrienoic acid analog protects pulmonary artery smooth muscle cells from apoptosis via ROCK pathway. *Exp Cell Res* **316**:2340–2353.

Marino JP, Jr (2009) Soluble epoxide hydrolase, a target with multiple opportunities for cardiovascular drug discovery. *Curr Top Med Chem* **9**:452–463.

Morin C, Sirois M, Echavé V, Albadine R, and Rousseau E (2010) 17,18-epoxyeicosatetraenoic acid targets $PPAR_\gamma$ and p38 mitogen-activated protein kinase to mediate its anti-inflammatory effects in the lung: role of soluble epoxide hydrolase. *Am J Respir Cell Mol Biol* **43**:564–575.

Pabla N and Dong Z (2008) Cisplatin nephrotoxicity: mechanisms and renoprotective strategies. *Kidney Int* **73**:994–1007.

Pabla N and Dong Z (2012) Curtailing side effects in chemotherapy: a tale of PKCδ in cisplatin treatment. *Oncotarget* **3**:107–111.

Pabla N, Murphy RF, Liu K, and Dong Z (2009) The copper transporter Ctr1 contributes to cisplatin uptake by renal tubular cells during cisplatin nephrotoxicity. *Am J Physiol Renal Physiol* **296**:F505–F511.

Park MS, De Leon M, and Devarajan P (2002) Cisplatin induces apoptosis in LLC-PK1 cells via activation of mitochondrial pathways. *J Am Soc Nephrol* **13**:858–865.

Raingeaud J, Gupta S, Rogers JS, Dickens M, Han J, Ulevitch RJ, and Davis RJ (1995) Pro-inflammatory cytokines and environmental stress cause p38 mitogen-activated protein kinase activation by dual phosphorylation on tyrosine and threonine. *J Biol Chem* **270**:7420–7426.

Ramesh G and Reeves WB (2002) TNF-α mediates chemokine and cytokine expression and renal injury in cisplatin nephrotoxicity. *J Clin Invest* **110**:835–842.

Ramesh G and Reeves WB (2003) TNFR2-mediated apoptosis and necrosis in cisplatin-induced acute renal failure. *Am J Physiol Renal Physiol* **285**:F610–F618.

Ramesh G and Reeves WB (2005) p38 MAP kinase inhibition ameliorates cisplatin nephrotoxicity in mice. *Am J Physiol Renal Physiol* **289**:F166–F174.

Reed JC (2002) Apoptosis-based therapies. *Nat Rev Drug Discov* **1**:111–121.

Reed JC, Doctor K, Rojas A, Zapata JM, Stehlik C, Fiorentino L, Damiano J, Roth W, Matsuzawa S, and Newman R et al.; RIKEN GER Group; ; GSL Members (2003) Comparative analysis of apoptosis and inflammation genes of mice and humans. *Genome Res* **13** (6B):1376–1388.

Samali A, Zhivotovsky B, Jones D, Nagata S, and Orrenius S (1999) Apoptosis: cell death defined by caspase activation. *Cell Death Differ* **6**:495–496.

Segreto HR, Oshima CT, Franco MF, Silva MR, Egami MI, Teixeira VP, and Segreto RA (2011) Phosphorylation and cytoplasmic localization of MAPK p38 during apoptosis signaling in bone marrow granulocytes of mice irradiated in vivo and the role of amifostine in reducing these effects. *Acta Histochem* **113**:300–307.

Seth R, Yang C, Kaushal V, Shah SV, and Kaushal GP (2005) p53-dependent caspase-2 activation in mitochondrial release of apoptosis-inducing factor and its role in renal tubular epithelial cell injury. *J Biol Chem* **280**:31230–31239.

Spector AA, Fang X, Snyder GD, and Weintraub NL (2004) Epoxyeicosatrienoic acids (EETs): metabolism and biochemical function. *Prog Lipid Res* **43**:55–90.

Tsuruya K, Ninomiya T, Tokumoto M, Hirakawa M, Masutani K, Taniguchi M, Fukuda K, Kanai H, Kishihara K, and Hirakata H et al. (2003) Direct involvement

of the receptor-mediated apoptotic pathways in cisplatin-induced renal tubular cell death. *Kidney Int* **63**:72–82.
Wang YX, Ulu A, Zhang LN, and Hammock B (2010) Soluble epoxide hydrolase in atherosclerosis. *Curr Atheroscler Rep* **12**:174–183.
Wei Q, Dong G, Franklin J, and Dong Z (2007) The pathological role of Bax in cisplatin nephrotoxicity. *Kidney Int* **72**:53–62.
Wolter KG, Hsu YT, Smith CL, Nechushtan A, Xi XG, and Youle RJ (1997) Movement of Bax from the cytosol to mitochondria during apoptosis. *J Cell Biol* **139**: 1281–1292.
Wood CD, Thornton TM, Sabio G, Davis RA, and Rincon M (2009) Nuclear localization of p38 MAPK in response to DNA damage. *Int J Biol Sci* **5**:428–437.
Yang S, Lin L, Chen JX, Lee CR, Seubert JM, Wang Y, Wang H, Chao ZR, Tao DD, and Gong JP et al. (2007) Cytochrome P-450 epoxygenases protect endothelial cells from apoptosis induced by tumor necrosis factor-α via MAPK and PI3K/Akt signaling pathways. *Am J Physiol Heart Circ Physiol* **293**:H142–H151.
Yao X, Panichpisal K, Kurtzman N, and Nugent K (2007) Cisplatin nephrotoxicity: a review. *Am J Med Sci* **334**:115–124.
Zhan Y, van de Water B, Wang Y, and Stevens JL (1999) The roles of caspase-3 and bcl-2 in chemically-induced apoptosis but not necrosis of renal epithelial cells. *Oncogene* **18**:6505–6512.
Zhang B, Ramesh G, Norbury CC, and Reeves WB (2007) Cisplatin-induced nephrotoxicity is mediated by tumor necrosis factor-alpha produced by renal parenchymal cells. *Kidney Int* **72**:37–44.
Zhao G, Tu L, Li X, Yang S, Chen C, Xu X, Wang P, and Wang DW (2012) Delivery of AAV2-CYP2J2 protects remnant kidney in the 5/6-nephrectomized rat via inhibition of apoptosis and fibrosis. *Hum Gene Ther* **23**:688–699.
Zhivotovsky B, Samali A, Gahm A, and Orrenius S (1999) Caspases: their intracellular localization and translocation during apoptosis. *Cell Death Differ* **6**: 644–651.

Address correspondence to: Dr. Deanna L. Kroetz, 1550 4th St., Box 2911, San Francisco, CA 94158-2911. E-mail: deanna.kroetz@ucsf.edu